Heliyon 10 (2024) e31360

Contents lists available at ScienceDirect

Heliyon

journal homepage: www.cell.com/heliyon

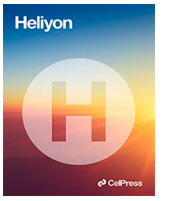

Research article

Potential use of a bone tissue engineering scaffold based on electrospun poly (ε-caprolactone) - Poly (vinyl alcohol) hybrid nanofibers containing modified cockle shell nanopowder

Kimiya Rahmani [a], Payam Zahedi [a,**], Mohsen Shahrousvand [b,*]

[a] Nano-Biopolymers Research Laboratory, School of Chemical Engineering, College of Engineering, University of Tehran, P.O. Box: 11155-4563, Tehran, Iran

[b] Caspian Faculty of Engineering, College of Engineering, University of Tehran, P.O. Box 119-43841, Chooka Branch, Rezvanshahr, 4386156387, Guilan Province, Iran

ARTICLE INFO

Keywords:
Poly (ε-caprolactone) (PCL)
Poly (vinyl alcohol) (PVA)
Cockle shell (CS)
Scaffold
Bone tissue

ABSTRACT

Today, the construction of scaffolds promoting the differentiation of stem cells is an intelligent innovation that accelerates the differentiation toward the target tissue. The use of calcium and phosphate compounds is capable of elevating the precision and efficiency of the osteogenic differentiation of stem cells. In this research, osteoconductive electrospun poly (ε-caprolactone) (PCL) - poly (vinyl alcohol) (PVA) hybrid nanofibrous scaffolds containing modified cockle shell (CS) nanopowder were prepared and investigated. In this regard, the modified CS nanopowder was prepared by grinding and modifying with phosphoric acid, and it was then added to PVA nanofibers at different weight percentages. Based on the SEM images, the optimum content of the modified CS nanopowder was set at 7 wt %, since reaching the threshold of agglomeration restricted this incorporation. In the second step, the PVA-CS7 nanofibrous sample was hybridized with different PCL ratios. Concerning the hydrophilicity and mechanical strength, the sample named PCL50-PVA50-CS7 was ultimately selected as the optimized and suitable candidate scaffold for bone tissue application. The accelerated hydrolytic degradation of the sample was also studied by FTIR and SEM analyses, and the results confirmed that the mineral deposits of CS are available approximately 7 days for mesenchymal stem cells. Moreover, Alizarin red staining illustrated that the presence of CS in the PCL50-PVA50-CS7 hybrid nanofibrous scaffold may potentially lead to an increase in calcium deposits with high precipitates, authenticating the differentiation of stem cells towards osteogenic cells.

1. Introduction

Bone is the strongest tissue in the body that can be damaged by a wide range of diseases, osteoporosis, trauma, and various cancers. While some of these injuries can be treated with common medical methods, a large number are incurable [1]. These are usually lesions

* Corresponding author. Caspian Faculty of Engineering, College of Engineering, University of Tehran, P.O. Box 43841-119, Guilan, Rezvanshar, Iran.

** Corresponding author. Nano-Biopolymers Research Laboratory, School of Chemical Engineering, College of Engineering, University of Tehran, P.O. Box: 11155-4563, Tehran, Iran.

E-mail addresses: phdzahedi@ut.ac.ir (P. Zahedi), m.shahrousvand@ut.ac.ir (M. Shahrousvand).

https://doi.org/10.1016/j.heliyon.2024.e31360
Received 22 October 2023; Received in revised form 14 May 2024; Accepted 15 May 2024
Available online 16 May 2024

in which part of the bone tissue is destroyed and the natural mechanisms in the body are unable to regenerate the damaged tissues. Bone is made up of a solid organic mold or matrix that is reinforced by the deposition of calcium salts and its cell culture on porous polymer scaffolds could be an efficient solution for bone tissue engineering applications [2,3].

Nanofibrous scaffolds are an excellent option for regenerating and repairing bone tissue damages and inconveniences by creating a suitable artificial environment for cell growth and proliferation [4,5]. The high surface-to-volume ratio of nanofibers increases the binding and proliferation of cells on nanofibers. A suitable scaffold for bone tissue must have sufficient porosity for cell migration, surface chemistry suitable for adhesion and growth and proliferation of cells, a degradation rate proportional to the rate of normal tissue regeneration, and a suitable nanofiber diameter to adapt to the physiological functions of the body [6]. Electrospinning is a common method for preparing nanofibrous scaffolds with nanometer and micrometer fibers, which can provide a structure similar to the extracellular matrix and a suitable environment for cell migration, adhesion, growth, and proliferation [7]. Various polymers have been used in the construction of electrospun scaffolds, but polymers from the group of poly(α-hydroxyl acid) such as poly (ε-caprolactone) (PCL), poly (glycolic acid), poly (lactic acid) were reported to be the most widely used in bone tissue systems [8,9]. PCL is a synthetic biocompatible, and biodegradable polymer with good mechanical properties. Since the PCL has a low melting temperature of 55–60°C, it can be easily shaped using various manufacturing methods [10]. Although, it has inadequate cell adhesion due to its lack of osteogenic properties and hydrophobic surface, incorporating inorganic substances or hydrophilic polymers into the PCL scaffold is a common way to enhance its hydrophilicity which can support the growth and differentiation of many cell types such as osteoblasts [11].

Researchers found that despite their good properties, many polymers could not be effective in bone regeneration alone. Since the bone tissue is strong and flexible, biological materials, like polymers and prestigious inorganic materials, are suggested to be combine and utilized for mimicking the behavior of natural tissue. For this purpose, to improve hydrophilicity, cell adhesion, and increase the degradation rate of PCL, its hybrid with hydrophilic substances such as PVA has been used [12]. One of the reasons for choosing PVA is due to its good solubility in cell culture medium at body temperature, which can easily release calcium deposits within itself and provide cells to differentiate [13]. In recent years, researchers have been able to reduce the contact angle on the PCL and hydrophilize the scaffold surface to allow for cell growth and proliferation by preparing a PVA-PCL hybrid [14].

In addition to polymers, other materials can also be incorporated into electrospun scaffolds for bone tissue engineering (BTE) such as hydroxyapatite, tricalcium phosphate, and other calcium derivatives [15–17]. The positive point of calcium phosphates is biocompatibility, which results in the formation of a layer rich in calcium and phosphorus on the surface of these substances [18,19]. Recent studies have shown that the use of calcium derivations, especially calcium phosphate ceramics such as HA along with polymers, in addition to creating better mechanical properties, also increases the degree of biocompatibility and bone formation. Due to the high commercial cost of calcium phosphates, natural compounds such as eggshell, cockle shell, etc. as green nano materials can be used with biological origin and low cost [20–23]. Cockle shells (CS) are naturally composed of 96 % calcium carbonate with small amounts of minerals. The presence of these trace elements makes it have a bone-like crystal composition and structure. So, cockle shell is a viable alternative to bone minerals for tissue engineering applications due to its porosity, non-toxicity, and biodegradability. Didekhani et al. incorporated oyster shell (OS) as a natural biomaterial for the first time to develop PCL/OS composite electrospun nanofiber scaffolds for BTE applications. The presence of oyster shells was found to be useful for more cell adhesion, osteogenic proliferation, and differentiation compared with pristine PCL [24]. CS can positively impact the bone differentiation of cells. Research indicates that calcium carbonate nanocrystals derived from cockle shells, specifically in the form of aragonite, enhance osteoblast function and differentiation. Studies have shown that these nanocrystals improve alkaline phosphatase activity, protein synthesis, and extracellular calcium deposition in osteoblasts [25]. The cell viability study suggests that these nanocrystals facilitate osteoblast differentiation and adhesion, leading to enhanced bone formation and mineralization.

This work is aimed at preparing novel PVA-CS nanofibers and their hybridization with PCL ones. After chemical modification of CS nanopowder, it is added to the CS nanofibers. On the other hand, PCL is inserted in the system to produce electrospun PCL-PVA-CS7 hybrid nanofibrous scaffolds. The potential osteogenic differentiation of the samples is evaluated by mesenchymal cell culture and results are investigated in detail.

2. Materials and methods

2.1. Materials

Poly (vinyl alcohol) (PVA, weight average molecular weight 80000 g mol^{-1}) was purchased from Nippon Gohsei (Japan). Poly (ε-caprolactone) (PCL, weight average molecular weight 98000 Da) was supplied from Sigma-Aldrich (USA). Chloroform, dimethyl formaldehyde (DMF), phosphoric acid, glutaraldehyde, acridine orange (AO), ethidium bromide (EB) and dimethyl sulfoxide (DMSO) were all provided from Merck Co., (Germany) and used without further purification. DMEM-F12 (Dulbecco's Modified Eagle Medium/ Nutrient Mixture F-12) cell culture medium from Gibco was used. MTT (3-(4,5-dimethylthiazol-2-yl)-2,5- diphenyltetrazolium bromide) assay, calcium content and alkaline phosphatase kits were all prepared from Pars Azmoon Co., (Iran).

2.2. Preparation of CS nanopowder

CS was collected from the Caspian Sea (Iran), pulverized in a ball mill after washing, and modified chemically as follows: 28 g of CS were added to 42 mL of phosphoric acid diluted by 500 mL of distilled water and stirred at 300 rpm. Then, the turbid solution was centrifuged at 3000 rpm for 4 min to separate the unreacted contents. The sediments were poured into a Petri dish and dried in an oven

at 70 °C for 24 h. Finally, the prepared white CS nanopowder was passed through a 450 nm syringe filter for size uniformity.

2.3. Preparation of electrospun PVA-CS nanofibers

A solution of PVA in distilled water (8 wt %) was prepared at a temperature of 70 °C based on the previous work [26]. To prepare PVA nanofibers containing modified CS nanopowder, the predetermined amounts of nanopowder were dispersed in distilled water, ultra-sonicated, and PVA was added to them (1, 3, 5, 7 wt %). Finally, the prepared solutions were electrospun at a flow rate of 0.8 mL/h, a distance-to-collector of 12–18 cm, and a voltage of 12–18 kV.

2.4. Preparation of electrospun PCL nanofibers

PCL solutions in 9, 12, and 15 wt % were prepared in chloroform and DMF in a volume ratio of 7:3. Then electrospinning of nanofibers was done with a voltage of 19 kV and a distance-to-collector of 14.5 cm [27].

2.5. Preparation of electrospun PCL-PVA-CS hybrid nanofibers

After determining the optimal conditions for electrospinning of PCL and PVA-CS, these two nanofibers were hybridized together in ratios of 50/50, 25/75, and 75/25 by using co-electrospinning. The hybrid mats were cross-linked in the presence of glutaraldehyde (the saturated vapor of glutaraldehyde (25 %v/v) in a vacuum chamber at room temperature for about 11 h) and dried in a vacuum oven at 30 °C for 24 h that excess unreacted glutaraldehyde is removed from the scaffolds [28].

2.6. Dynamic light scattering

To measure CS nanopowder before and after passing through the 450 nm nozzle filter, a dynamic light scattering (DLS, SZ-100z, Horiba Jobin Jyovin Co., Japan) was utilized.

2.7. Fourier transform infrared spectroscopy

To evaluate the characteristic peaks of scaffolds at different times after hydrolytic degradation, a Fourier transform infrared spectroscopy (FTIR, Equinox 55, Bruker Co., United States) was employed with wavenumbers in the range of 500–4000 cm^{-1}.

2.7.1. Scanning electron microscopy

The morphology of the CS nanopowder and the nanofibers was observed by using a scanning electron microscope (SEM, MIRA II, Tescan Co., Czech). All samples were coated with thin layers of gold and the micrograph images were recorded at different magnifications.

2.8. Energy dispersive X-ray analysis

The presence of modified CS nanopowder in the nanofibers was studied by energy dispersive X-ray analysis (EDX, Tescan Co., Czech). For evaluation of the cross-section of nanofibers, after inserting them in the epoxy resin and drying, they were put in liquid nitrogen and broken perpendicular to the direction of nanofibers.

2.9. Water contact angle measurements

The water contact angle was measured by placing a drop of water on the surface of the scaffolds with a contact goniometer (WCA, Kruss Co., Germany) [29]. The contact angle measurements were performed three times for each scaffold and the average was reported.

2.10. Tensile test

Mechanical properties of the nanofibers were investigated using a tensile apparatus (5566, Instron, England). For this purpose, scaffolds with dimensions of 5 × 30 mm were cut and they were extended with a cross-head speed of 5 mm/min the average results were reported with three times repeat of this test. In order for the scaffolds to fit well in the tensile machine, they were placed in a paper frame and the frames were cut with scissors before performing the test (ASTM D3379) [30].

2.11. Porosity measurements

Digimizer software was used to calculate the circle equivalent of the pores from the SEM images. Then the porosity of each scaffold was calculated using the following Equation 1:

$$\textit{Surface porosity}\ (\%) = (A_P\ /\ A_T) \times 100 \quad (1)$$

where "A_P" and "A_T" are the average surface area of pores and the SEM image, respectively.

2.12. Accelerated hydrolytic degradation studies

The accelerated hydrolytic degradation of samples in sodium hydroxide (1 M) at 45 °C was investigated after 1, 3, 6, 12, 24, and 48 h [31,32]. They were washed several times with deionized water, dried again in a 45 °C oven for 24 h, and weighed. The residual weight is measured using the following Equation (2):

$$Reminding\ mass(\%) = 100 - \ ((Mi - Mf) \times 100)/Mi \quad (2)$$

where "M_i", "M_f" are weights of dry samples before and after degradation, respectively.

On the other hand, hydrolytic degradation was performed in a physical solution called phosphate buffer saline (PBS, pH 7.4) at 37 °C for 35 days. The remaining weight of scaffolds after degradation was calculated by Eq. (2). These measurements were done 3 times with a standard deviation < 5 %.

2.13. Cell culture

In this line, two groups were evaluated for cell viability and differentiation, one for PCL-PVA-CS scaffolds and the other for (50/50) scaffolds as a control sample. At first, scaffolds were sterilized and cut as a circle with a diameter of 0.5 cm, then placed inside the wells of a 24-cell culture container. Following this, up to 500 μL of culture medium (DMEM) containing 10 % bovine serum (FBS) was added to each well, and 10,000 cells were placed on each scaffold. The culture container was placed inside an incubator set at a temperature of 37 °C and 5 % carbon dioxide. At 1, 3, and 5 days after the initial culture, and at a specific hour, 50 μL of tetrazolium bromide MTT solution (5 mg mL^{-1} in a basic environment) were added to each well. The culture container was then returned to the incubator for 3 h.

2.13.1. Cell viability

MTT assay was performed by using Eq. (3) to evaluate the biocompatibility of electrospun PCL-PVA-CS nanofibers in the presence and absence of CS against fibroblast cell (L929) with numbers of 10^4 cell/well through 24 well-plate at 37 °C and 5 % of CO_2.

$$Relative\ cell\ viability(\%) = (OD\ /\ avg\ ODC') \times 100 \quad (3)$$

where "OD" is the absorbance value of samples and "avg ODC'" is the average absorbance value of the cell control.

2.13.2. Cell adhesion

After culturing fibroblast cells (L929) on PCL-PVA and PCL-PVA-CS nanofibers with and without CS. The cell adhesion was studied after 24 h by SEM images with magnifications of 1000× and 5500x.

2.13.3. Alkaline phosphatase

Alkaline phosphatase activity (ALP) activity was done in 7 and 14 days [33,34]. For this purpose, the first 100 μL of RIPA (Radioimmunoprecipitation assay) buffer solution were added to the cell culture medium containing the scaffold and control samples to remove the proteins from the cell. The contents of the wells were centrifuged (14000 rpm) for 15 min at 4 °C. Subsequently, 1 μL of (*p*)-nitrophenol phosphate solution was added to each sample and measured and by ELISA reader (3200 DANA, Garni Rizpardaz Co., Iran) at a wavelength of 450 nm.

2.13.4. Calcium content

This experiment is similar to the ALP test performed on days 14 and 21. Then 200 μL of 0.6 N hydrochloric acid solution was added and pipetted well and were eventually transferred to vials [34]. Then, a calcium content kit was used to measure the amount of calcium deposits. Finally, light absorption in the range of 750 nm with the laser was read (3200 DANA, Garni Rizpardaz Co., Iran).

2.13.5. Alizarin red staining

Alizarin red staining is a substance that selectively stains calcium deposits, and it has been utilized in recent times to examine calcium-rich deposits that are formed in cell cultures. In this method, after washing the differentiated cells with PBS, an appropriate amount of a 1 % alizarin red dye solution (by weight) was added to the cells for 5–10 min. Then, they were washed again with PBS, and their images were taken using a light microscope.

2.13.6. Statistical analysis

Data were expressed as mean value ± standard error. All the data were statistically analyzed by one-way analysis of variance (ANOVA) using IBM SPSS Statistics analysis of variance (20.0) and GraphPad Prism software. Statistical difference was considered significant when probability values were less than 0.05 ($p < 0.05$).

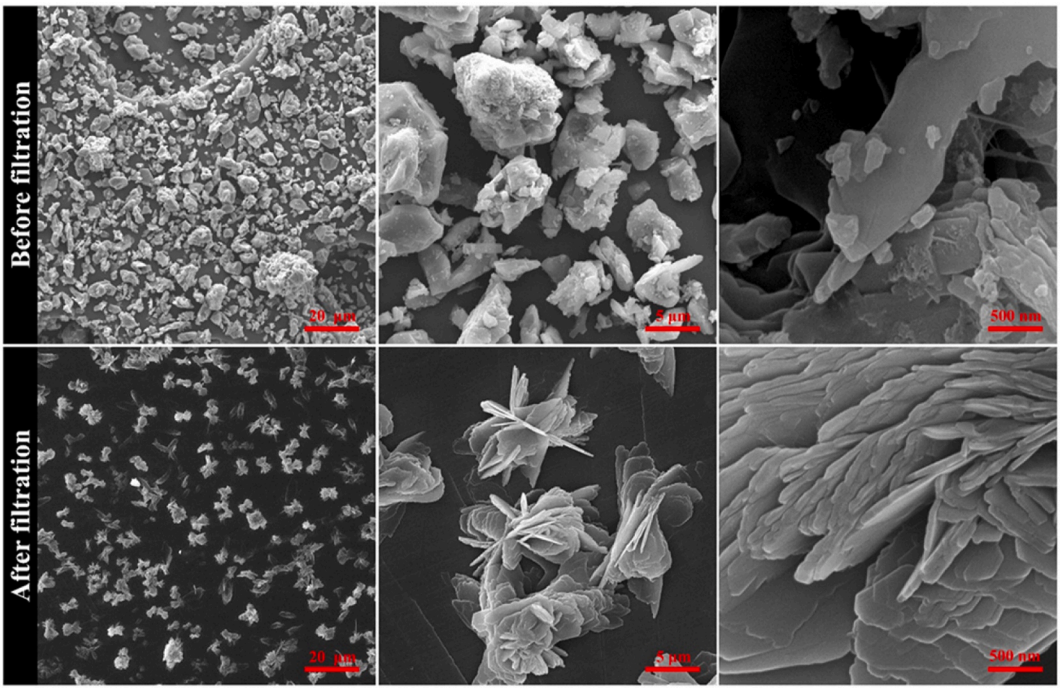

Fig. 1. SEM micrograph of CS nanopowder before and after filtration by a syringe filter with a 0.45 μm pore size.

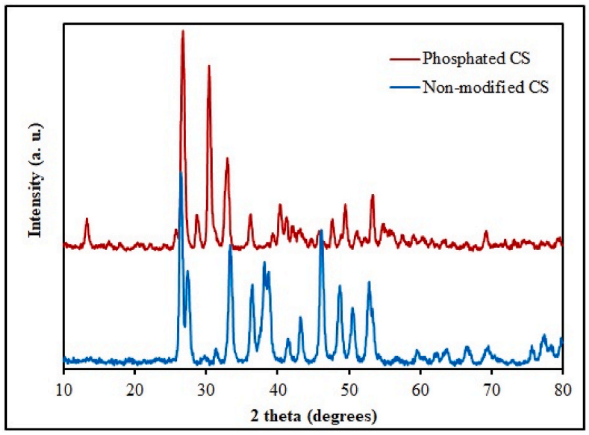

Fig. 2. XRD spectra raw cockle shell powder as non-modified CS and phosphated CS as modified CS.

3. Results and discussions

3.1. Evaluation of CS nanopowder

After grinding and modifying the CS nanopowder with phosphoric acid, its nanoparticles should be separated. For this purpose, a syringe filter with a 0.45 μm pore size was used. As the SEM images in Fig. 1 show, the size of the particles after filtering has become much smaller and more uniform than before filtering. Filtered CS nanoparticles have a plate morphology with a thickness of less than 100 nm. Of course, the results of the DLS test estimated the average diameter of the CS before and after filtration to be 300 and 1000 nm, respectively (Fig. S1). The difference between SEM and DLS results could be because the DLS test measures the radius of the gyration of the particles. The size range of cockle shell nanoparticles varies depending on the study. Reported dimensions include nanoparticles with sizes ranging from 0.5 to 3 nm in diameter and 20–1000 nm in length [35]. Additionally, other studies have reported average sizes of around 78.8 ± 10.8 nm [36], and 37.8±3–55.2 ± 9 nm [37] for cockle shell nanoparticles. The chemical structure of CS consists mainly of aragonite, which is a crystalline form of calcium carbonate (CaCO3). Shells are composed mainly of calcium, with minor amounts of magnesium, silicon, sodium, and other minerals. X-ray diffraction (XRD) analysis shown in Fig. 2

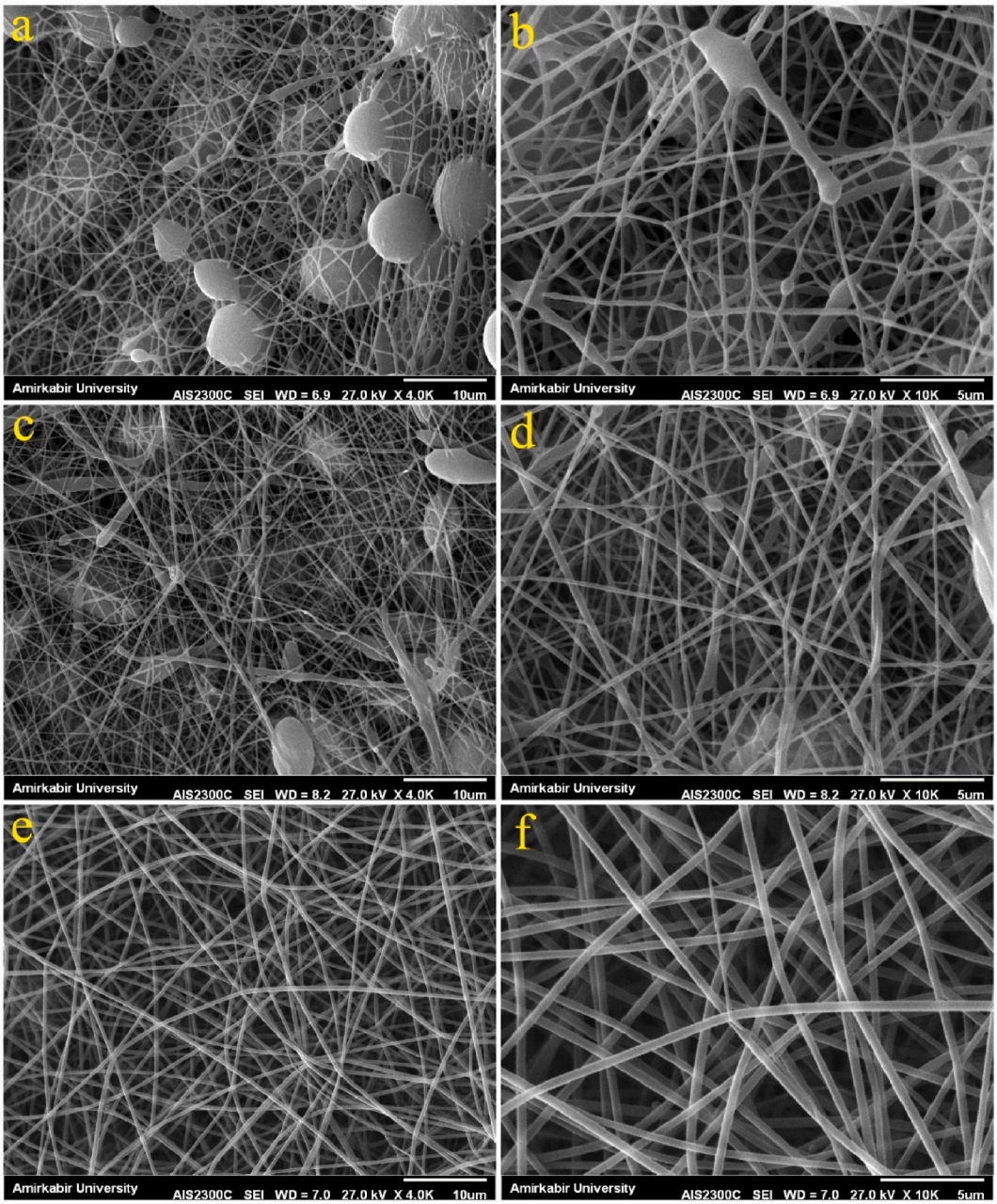

Fig. 3. SEM micrographs of electrospun PCL nanofibers for different concentrations: (a, b) 9 wt %, (c, d) 12 wt %, and (e, f) 15 wt % at two magnifications.

confirms that the CSs are mainly composed of aragonite, a specific polymorph of calcium carbonate [38]. The indicative peaks in the XRD analysis of the cockle shell include peaks at approximately $2\theta = 29.4^{\circ}$, 32°, 38°, 54°, 64°, and 68°. These peaks are significant in identifying the crystal structure and chemical composition of the material, particularly in determining the presence of calcite and aragonite phases [39,40]. The difference in the peaks in the graph of non-modified nanoparticles with phosphate CS nanoparticles is a confirmation of its successful modification, so that the peak in 13.4 shows the structure of $Ca_3(PO_4)_2$ [41].

3.2. Evaluation of electrospun PVA nanofibers containing modified CS

CS as an osteogenic agent causes differentiation in stem cells. The ossifying agent must be released from the scaffold at the appropriate time and made available to the cells for differentiation. On the other hand, the degradation and release of CS from PCL fibers are slow. Because PCL is a hydrophobic polyester whose hydrolytic degradation is slow [42]. Therefore, CS particles were added

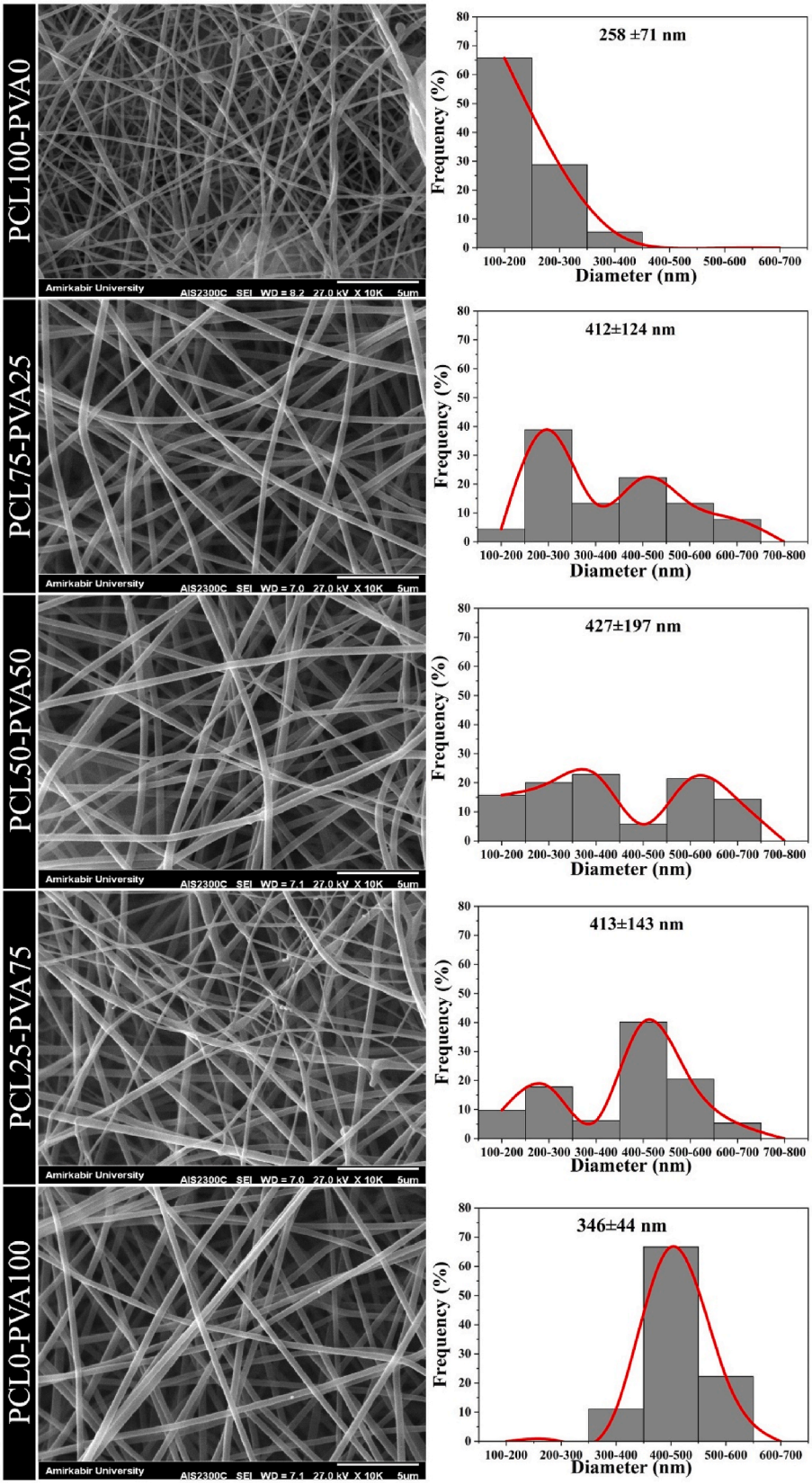

Fig. 4. SEM micrographs and nanofiber diameter distribution of PCL-PVA hybrids containing of CS.

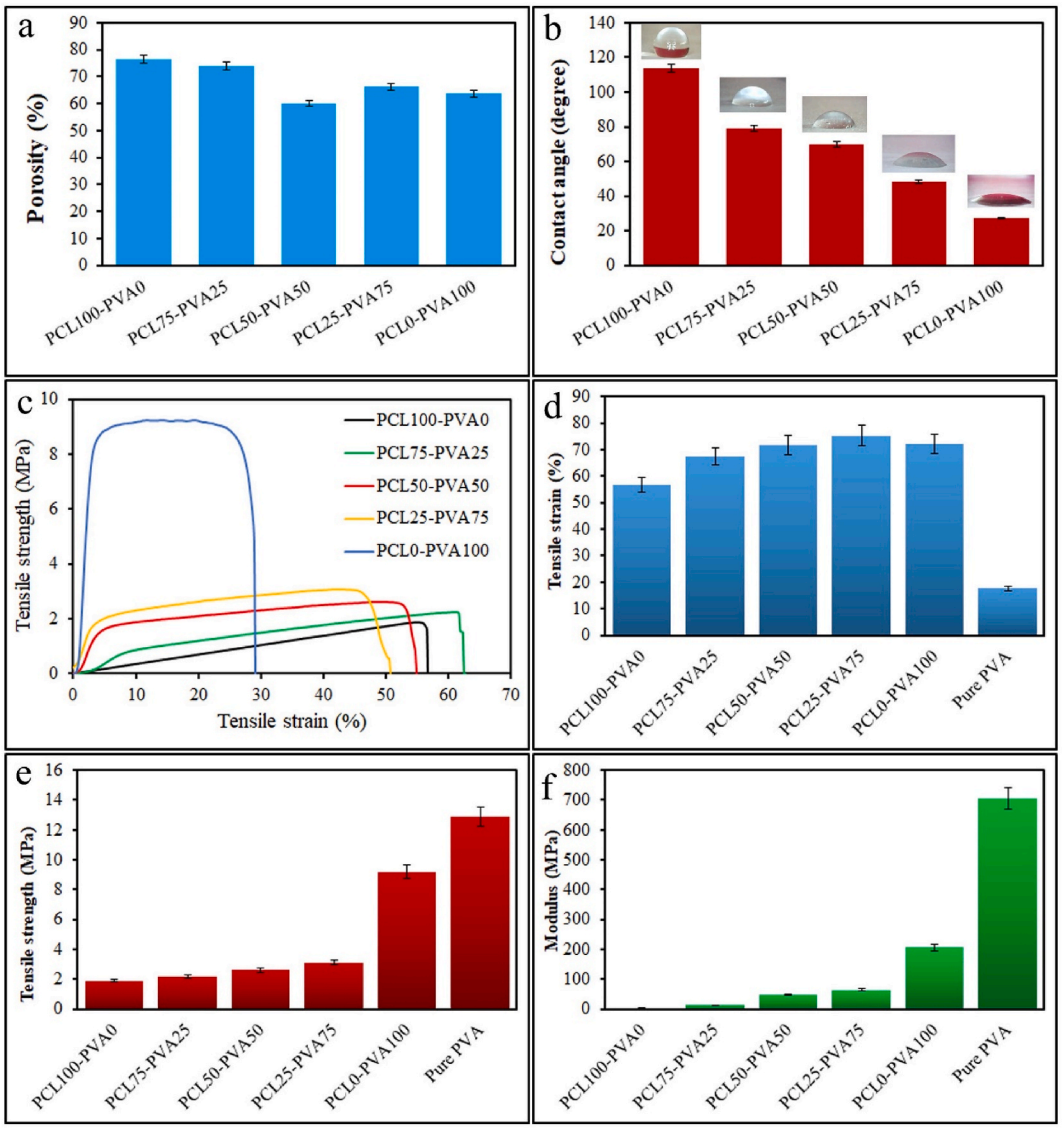

Fig. 5. (a) Porosity [58]; (b) Water contact angle; (c) mechanical analysis; (d) Tensile strain; (e) Tensile strength; (f) Modulus of PCL-PVA hybrids containing of CS.

to PVA. For this purpose, the electrospinning process of combining different percentages including 1, 3, 5 and 7 wt % of CS nanopowder in PVA solution was performed. Electrospinning with different voltages and distances at constant flow (0.8) mL/h was performed to find the best nanofibers. Fig. S2 shows the SEM microscope images of PVA-CS electrospun nanofibers. As can be seen, nanofibers containing 1, 3, and 5 wt % of CS are completely homogeneous and have any beads. However, by increasing the amount of CS nanoparticles up to 7 wt % due to the accumulation of CS nanoparticles, beads are formed [43,44]. Therefore, the threshold for adding CS nanoparticles is 7 wt % of PVA. Also, fiber diameter distribution diagrams show that with increasing weight CS, the average nanofiber diameter from 460 nm to 347 nm has changed (Fig. S3). To ensure the presence of CS in nanofibers, the EDX test was prepared from the cross-section of nanofibers. Fig. S4 shows the presence of calcium (blue dots) and phosphorus (orange dots) elements due to the proper dispersion of CS in PVA nanofibers.

3.3. Evaluation of electrospun PCL

To prepare PCL and PVA hybrid, the suitable conditions for each of these two polymers should be evaluated separately and the optimal electrospinning conditions should be determined for each. Previous research confirmed that PCL spun well in concentrations higher than 9 wt % [45]. Therefore, PCL was spun in three concentrations of 9, 12, and 15 wt % and their SEM images are shown in Fig. 3a–f.

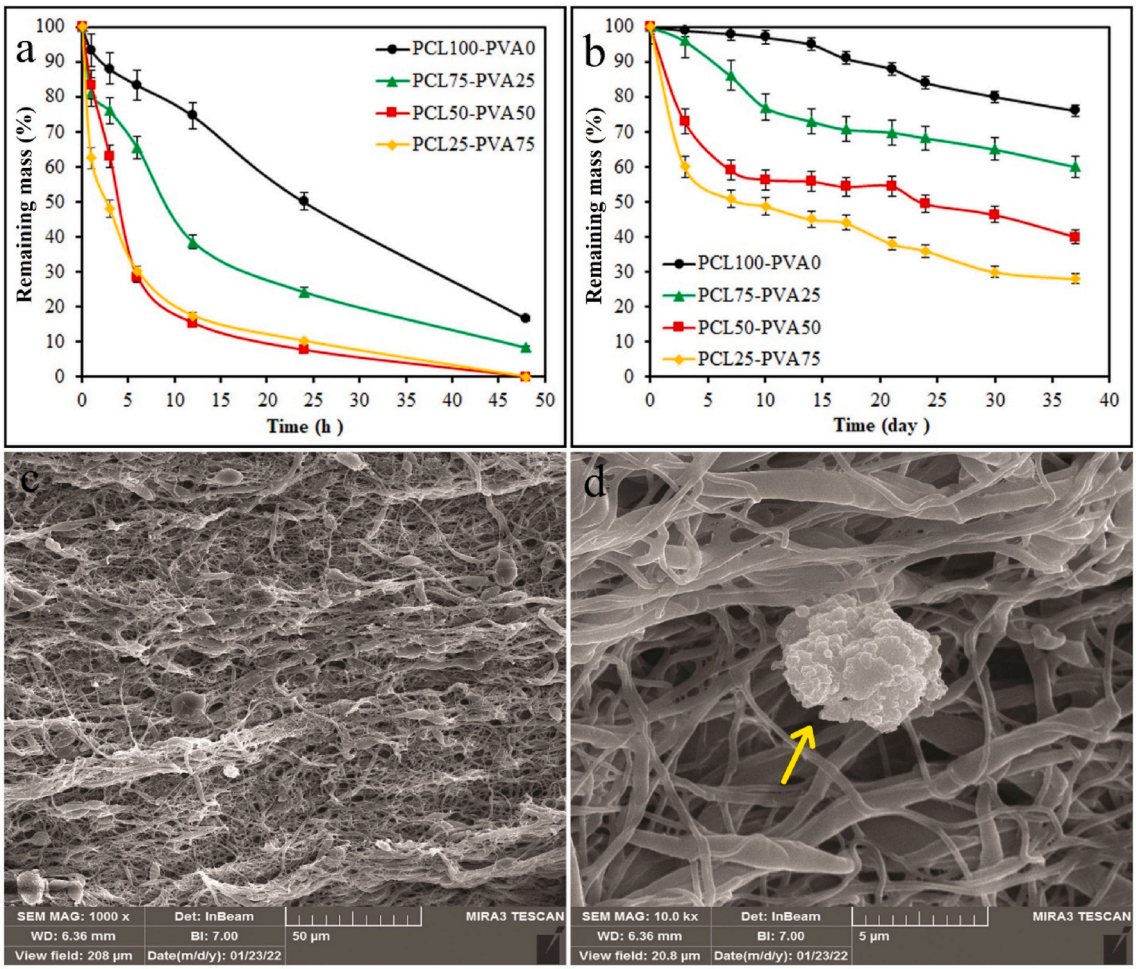

Fig. 6. (a) Accelerated degradation of electrospun PCL-PVA-CS hybrids; (b) Normal degradation of electrospun PCL-PVA-CS hybrids in PBS; (c, d) SEM micrograph of PCL50-PVA50-CS7 after the hydrolytic degradation in PBS solution.

The results showed that the nanofibers 9 and 12 wt % are mats with drops and beads. This is despite the fact that the nanofibers of PCL 15 % wt. do not have beads and are uniform. Of course, researchers have proven that the diameter of the nanofibers increases with increasing concentration of the solution [46]. In analyzing the diameter of electrospun nanofibers, attention should be paid to the balance of three main forces: viscoelasticity, surface charge, and surface tension. Viscoelasticity and surface tension are the restraining forces of nanofiber jumping. With the increase in polymer molecular mass and the same polymer concentration, these forces increase and lead to an increase in the diameter of the nanofibers and even create beads. While the surface charge is the driving force for jumping the nanofibers toward the collector. Since most polymers are conductive insulators, solvents with high dielectric constant are used to improve the surface charge. Also, increasing the voltage can increase the surface charge. Increasing of surface charge force can reduce the diameter of the nanofibers. If this force increases too much and the two restraining forces of viscoelasticity and surface tension decrease, the nanofibers are fragmented and the possibility of bead formation increases. Therefore, to have uniform and suitable nanofibers, there must be a balance between the promoting and hindering forces [8]. Therefore, in this research, the concentration of 15 % wt. of PCL is the equilibrium threshold of these nanofibers, and uniform nanofibers are obtained.

3.4. Evaluation of electrospun hybrids PCL-PVA-CS7

After determining the optimal electrospinning conditions of PCL and PVA, the hybrid of these nanofibers was spun in the combination of 0, 25, 50, 75, and 100 %. The SEM of electrospun hybrids and their diameter distribution diagrams are shown in Fig. 4. As is seen, the scaffolds have no beads and the diagrams show a twin nanofiber diameter distribution of two polymers. For the 25 % PCL75-PVA25 scaffold, which has more PCL, the peak at 200 nm is more intense, and for the PCL25-PVA75, the peak at 400 nm is more intense. On the other hand, PCL50-PVA50 hybrids show relatively equal peak intensity of two polymers. The porosity of electrospun scaffolds was about 60 % as shown in Fig. 5a sufficient porosity is one of the most important features of bone scaffolds for cell growth, proliferation, and migration. Porosity increases surface area to volume, facilitates accurate growth and distribution of cells throughout

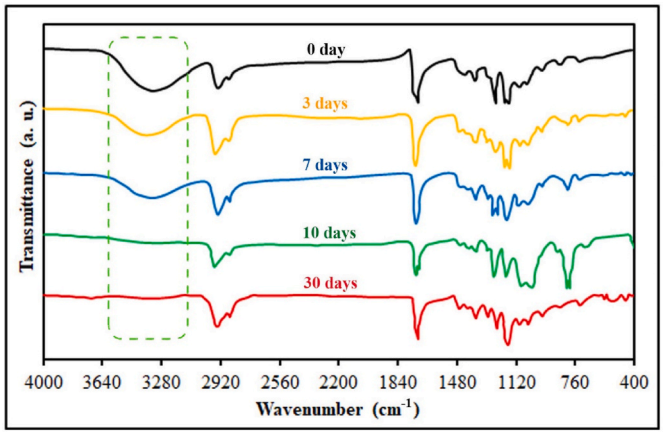

Fig. 7. FTIR spectrum of PCL50-PVA50-CS degraded scaffolds in PBS solution within 30 days.

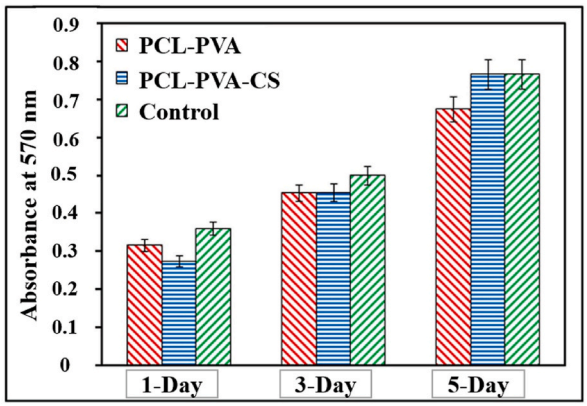

Fig. 8. Cell viability evaluation of fibroblast cells (L929) cultured on PCL50-PVA50 and PCL50-PVA50-CS7 nanofibers for 1, 3 and 5 days.

the scaffold, and the formation of blood vessels around new tissue. Porosity also plays an important role in the release of food, oxygen, and waste. It should be noted mechanical strength may decrease with increasing porosity percentage. Maheshwari et al. also reported hybrid porosity of 59 % and 64 %, which is a good porosity for bone tissue applications [14]. As it is clear from the SEM images, the pore size of the scaffolds is around 5–20 μm. The dimensions of an osteoblast cell typically range from 5 to 20 μm in diameter [47]. The outer cell membrane contains OH functional groups. For this reason, cells have better adhesion, growth, and proliferation on the hydrophilic surface. Therefore, the prepared bone scaffold should be made of hydrophilic polymers or modified in various ways for this purpose. PCL is an absorbent polymer with a water contact angle of 114° [48,49].

When PCL is hybridized with different amounts of PVA, its hydrophilicity is improved (Fig. 5b). The scaffolds must be able to protect the cells against compressive and tensile strength. The mechanical properties of prepared scaffolds were investigated (Fig. 5c–f). PCL is a tough polymer that has a higher elongation rate compared to PVA. But the modulus and strength of PVA is higher than PCL. Therefore, in the hybrids prepared by increasing the amount of PVA, the increase in length decreased and the modulus and final strength of the scaffolds increased. Degradability of scaffolds is one of their requirements. Therefore, the degradability of the prepared scaffolds was investigated in two different conditions (Fig. 6 a, b). The degradability test is a time-consuming test, so this feature was first checked by an accelerated test, and then the main test was also performed [50,51].

Although PCL is an ester polymer and prone to degradation, it degrades slowly due to its hydrophobicity. Therefore, hybridizing this polymer with PVA has led to an increase in its degradability rate. The results confirmed that by increasing the amount of PVA, the degradability of the prepared hybrids improved. SEM images after the hydrolytic degradation of the scaffolds in the buffer environment are shown in Fig. 6, PCL50-PVA50 was selected as the optimal scaffold for further evaluation due to its suitable hydrophilicity and mechanical strength. The interesting point is that after the dissolution of PVA, CS nanopowder were released and formed calcium deposits on the scaffold (Fig. 6 c, d). Creation of mineral deposits in scaffolds is one of the key parameters of bone differentiation of stem cells. The question is, after how many days these mineral deposits are available to the stem cells? The scaffolds were placed in the buffer environment and were removed from the solution on different days and evaluated by FTIR after drying (Fig. 7).

The FTIR analysis of PCL and PVA electrospun fibers reveals distinct peaks corresponding to different functional groups present in the materials. In the FTIR spectra of PVA fibers, characteristic peaks are observed at 3267 cm^{-1} (O–H stretching), 2915 cm^{-1} (C–H

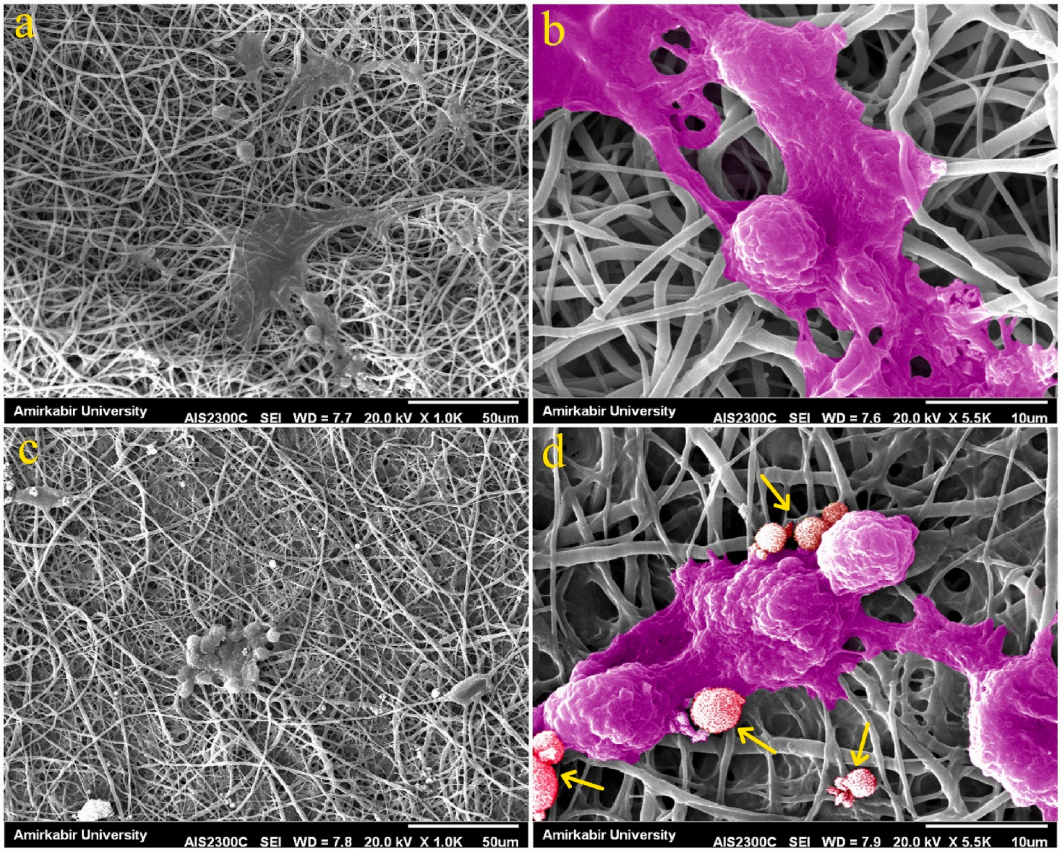

Fig. 9. Cell adhesion on (a, b) PCL50-PVA50 without CS and (c, d) PCL50-PVA50 containing CS in two magnifications (This is post-processing).

stretching), 1708 cm^{-1} (carbonyl group C═O stretching), and 1220 cm^{-1} (ester group stretching). On the other hand, the FTIR spectra of PCL fibers exhibit peaks at 2942 cm^{-1} (CH_2 asymmetric stretching), 2865 cm^{-1} (CH_2 symmetric stretching), 1720 cm^{-1} (carbonyl group stretching), and 1366 cm^{-1} (CH_2 bending vibrations) [52]. The results confirmed PVA has completely dissolved after 7 days. Therefore, mineral deposits will be available to stem cells in less than 7 days. As can be seen, after 7 days PVA becomes degraded, and CS is released. As hMSCs that differentiate to osteoblast typically proliferate between 7 and 14 days, so minerals like CS can be easily accessible to cells during this period. After that, during 14–30 days it differentiates [53].

3.5. Cell viability and cell adhesion

The MTT method is used to evaluate cell viability and proliferation of L929 fibroblasts cultured on the PCL50-PVA50 and PCL50-PVA50-CS7 scaffolds for 5 days. The results confirmed that the biocompatibility of all samples was higher than 85 % compared to the control sample (Fig. 8). Also, there is no significant difference between the results. Although PCL-50-PVA50-CS7 is slightly lower than the control sample on days 1 and 3, it has reached 100 % biocompatibility on day 5. This issue can be due to the roughness on the surface of the scaffolds due to the remaining mineral deposits after the dissolution of PVA. These results are consistent with what was observed in the degradability test (Fig. 6c–d and Fig. 7). Percentages of cell viability above 80 % are considered non-cytotoxic, between 80 % and 60 % is classified as weak cytotoxicity, from 60 % to 40 % is categorized as moderate cytotoxicity, and below 40 % is classified as strong cytotoxicity [50,54]. Therefore, scaffolds containing CS nanopowder have increased the possibility of cell adhesion [55]. The SEM images of the cells fixed on the scaffolds in Fig. 9a–d confirm this. The cells adhered well on both PCL50-PVA50 and PCL50-PVA50-CS7 samples. An interesting point to note is the presence of aggregations of CS nanoparticle deposits around the attached cells on the PCL50-PVA50-CS7, which is consistent with the analysis of the biocompatibility test results. This feature can have a direct effect on the bone differentiation of stem cells.

3.6. Osteogenic differentiation of hMSCs on PCL50-PVA50-CS7 scaffolds

ALP assay, calcium content (CPC), and alizarin red staining were conducted to evaluate the effect of CS nanoparticles in the scaffolds on the ossification behavior of the electrospun mats (Fig. 10). Evaluation of alkaline phosphatase activity as a primary marker of bone cells determines the ability of nanofiber scaffolds to differentiate bone marrow from mesenchymal stem cells [56]. The

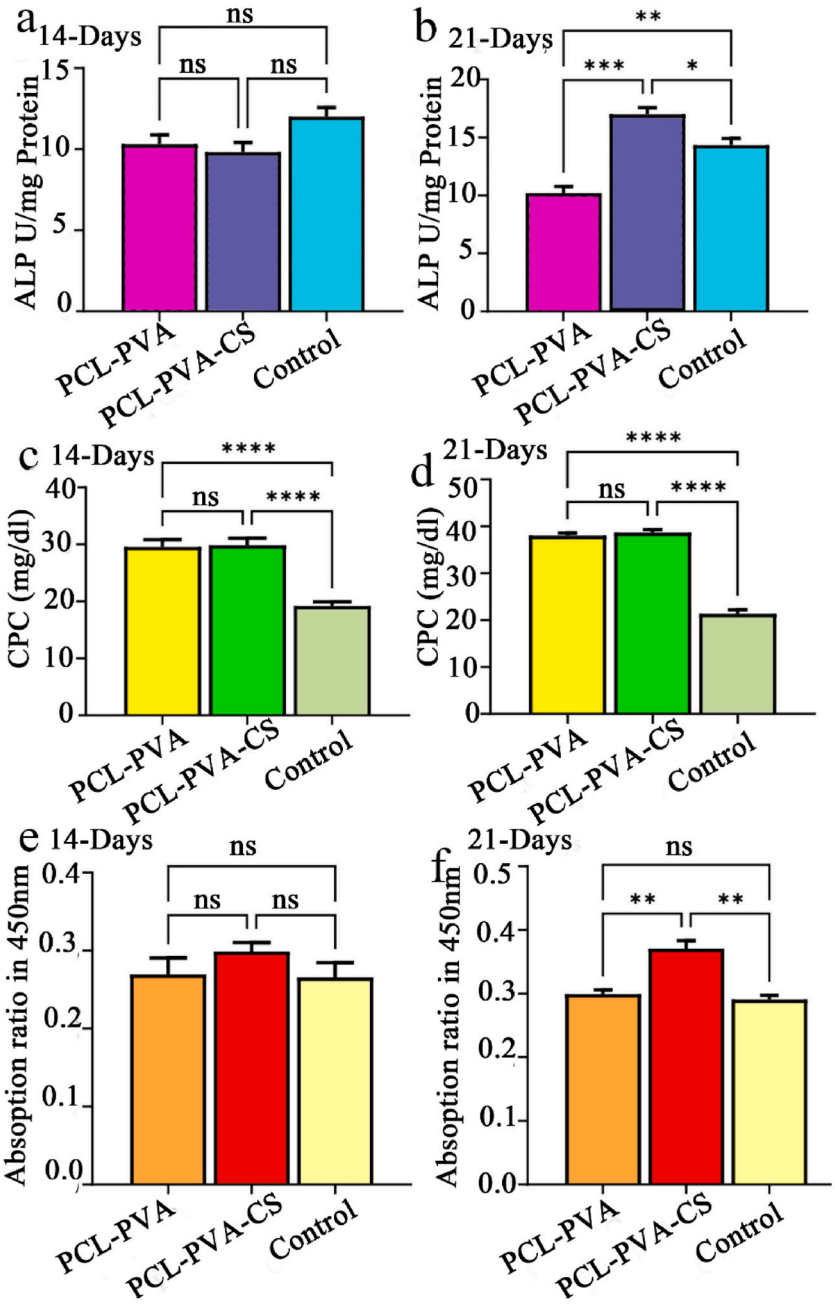

Fig. 10. Osteogenic differentiation of MSCs on PCL50-PVA50 and PCL50-PVA50-CS7: (a, b) ALP activity; (c, d) Calcium content (CPC); (e, f) Alizarin red staining colorimetry(****: $p < 0.05$, ns: not significant). (For interpretation of the references to color in this figure legend, the reader is referred to the Web version of this article.)

enzymatic activity of PCL50-PVA50 and PCL50-PVA50-CS7 scaffolds was examined on days 14 and 21 (Fig. 10 a, b). There is a significant difference between the control and 2 groups of scaffolds. While both samples, especially the PVA sample, showed a significant difference with the control on the 21st day. These result display that the presence of CS as inorganic bioactive component in the PCL-PVA scaffold, could greatly accelerate the osteogenic differentiation of MC3T3 cells. Maheshwari et al. examined the level of enzymatic activity after cell seeding bone marrow cells on a PCL-PVA-HA scaffolds [14]. The results showed that the amount of enzymatic activity on the scaffold containing HA was significantly different from the other samples (Fig. 10c and d). In fact, it shows the effective presence of inorganic component in osteogenic differentiation. There was no significant difference between CPC result of PCL-PVA and PCL-PVA-CS7 scaffolds on both 14 and 21days ($P > 0.05$). However, there was higher levels in calcium deposition of both groups compared with the control sample (Fig. 10e and f). As can be seen the difference between 14 and 21 days, over the time,

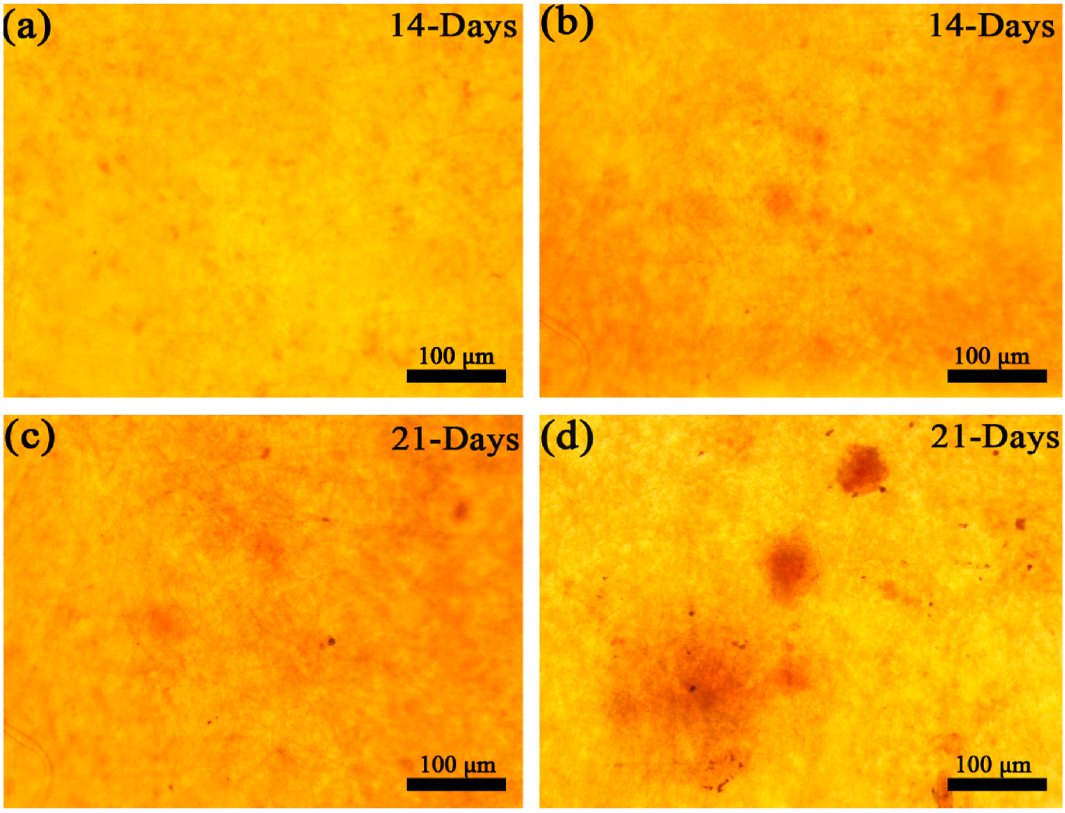

Fig. 11. Alizarin red staining of osteogenic differentiation of hMSC; (a, b) for PCL50-PVA50 nanofibers, (c, d) for PCL50-PVA50-CS7 after 14 and 21 days. (For interpretation of the references to color in this figure legend, the reader is referred to the Web version of this article.)

formation of calcium deposits on scaffolding has increased, which shows the level of differentiation of hMSCs is increasing. In previous studies, it has been proved that the organic matrix of CS has the ability to initiate the differentiation and proliferation of osteoblasts due to having diffusible molecules [57]. Alizarin red staining was utilized to discover the mineralization on nanofiber scaffolds confirming the osteogenic process. The results of this test also show that the PCL50-PVA50-CS7 scaffolds on the 21st day had a significant effect on the formation of calcium deposits caused by bone differentiation.

Fig. 11a–d indicates after being exposed to osteogenic differentiation medium for 14 and 21 days, the cells formed deposits on the PCL50-PVA50 and PCL50-PVA50-CS7 scaffolds that were rich in calcium. Subsequently, presence of CS nanoparticles in scaffolds promotes bone growth.

4. Conclusion

The purpose of this research was to prepare a bone tissue engineering scaffold that has stimulating properties for better and faster differentiation of stem cells. For this purpose, PVA has been used to improve the hydrophilicity of the scaffold, and CS powder has been used as a green nanomaterial for faster differentiation of stem cells. In summary, electrospun nanofibers PCL-PVA containing 7 % modified CS were prepared. The XRD analysis from CS determined that the chemical composition of CS was aragonite. The results showed that the optimal amount of CS in PVA electrospun fibers was around 7 wt%, and the fibers did not suffer from aggregates or beads. Further, the FTIR test confirmed that these nanoparticles are well released in less than 10 days in the aqueous medium and can be easily accessible to the stem cells. The results of the mechanical test showed that the increase in PVA can lead to an increase in the mechanical strength of electrospun scaffolds hybridized with PCL. When PCL is hybridized with different amounts of PVA, its hydrophilicity is improved. PCL and PVA hybrid scaffolds in a ratio of 50-50 of both polymers have a contact angle of 70°, which is hydrophilic compared to PCL, which is 114°. ALP assay, calcium content (CPC), and alizarin red staining as confirmatory tests of osteogenic differentiation of stem cells showed that the presence of nanoparticles had a significant effect on the differentiation process. Based on this research, it can be concluded that the PCL-PVA-CS7 scaffold could be assumed as a bone scaffold for bone tissue engineering.

CRediT authorship contribution statement

Kimiya Rahmani: Writing – original draft, Methodology, Data curation. **Payam Zahedi:** Writing – review & editing, Writing –

original draft, Supervision, Methodology, Investigation, Funding acquisition, Data curation. **Mohsen Shahrousvand:** Writing – review & editing, Writing – original draft, Supervision, Methodology, Investigation, Data curation.

Declaration of competing interest

The authors declare that they have no known competing financial interests or personal relationships that could have appeared to influence the work reported in this paper.

Acknowledgements

The authors would like to thank the Laboratory of the Faculty of Chemical Engineering at the University of Tehran for their partial support of this work.

Appendix A. Supplementary data

Supplementary data to this article can be found online at https://doi.org/10.1016/j.heliyon.2024.e31360.

References

[1] F.R. Maia, A.R. Bastos, J.M. Oliveira, V.M. Correlo, R.L. Reis, Recent approaches towards bone tissue engineering, Bone 154 (2022) 116256.
[2] P. Ghaffari-Bohlouli, P. Zahedi, M. Shahrousvand, Enhanced osteogenesis using poly (l-lactide-co-d, l-lactide)/poly (acrylic acid) nanofibrous scaffolds in presence of dexamethasone-loaded molecularly imprinted polymer nanoparticles, Int. J. Biol. Macromol. 165 (Pt B) (2020) 2363–2377.
[3] G. Borciani, T. Fischetti, G. Ciapetti, M. Montesissa, N. Baldini, G. Graziani, Marine biological waste as a source of hydroxyapatite for bone tissue engineering applications, Ceram. Int. 49 (2) (2023) 1572–1584.
[4] S. Chahal, A. Kumar, F.S.J. Hussian, Development of biomimetic electrospun polymeric biomaterials for bone tissue engineering. A review, J. Biomater. Sci. Polym. Ed. 30 (14) (2019) 1308–1355.
[5] E. Ahmadian, A. Eftekhari, D. Janas, P. Vahedi, Nanofiber scaffolds based on extracellular matrix for articular cartilage engineering: a perspective, Nanotheranostics 7 (1) (2023) 61.
[6] L. Suamte, A. Tirkey, J. Barman, P.J. Babu, Various manufacturing methods and ideal properties of scaffolds for tissue engineering applications, Smart Mater Manuf 1 (2023) 100011.
[7] A. Jalali Jahromi, M. Mirhosseini, H. Molla Hoseini, H. Nikukar, A review on commonly used scaffolds in tissue engineering for bone tissue regeneration, J Sadoughi Uni Med Sci (2020).
[8] M. Shahrousvand, V. Haddadi-Asl, M. Shahrousvand, Step-by-step design of poly (epsilon-caprolactone)/chitosan/Melilotus officinalis extract electrospun nanofibers for wound dressing applications, Int. J. Biol. Macromol. 180 (2021) 36–50.
[9] P. Ghaffari-Bohlouli, M. Shahrousvand, P. Zahedi, M. Shahrousvand, Performance evaluation of poly (l-lactide-co-D, l-lactide)/poly (acrylic acid) blends and their nanofibers for tissue engineering applications, Int. J. Biol. Macromol. 122 (2019) 1008–1016.
[10] M.I. Hassan, N. Sultana, S. Hamdan, Bioactivity assessment of poly(ε-caprolactone)/hydroxyapatite electrospun fibers for bone tissue engineering application, J. Nanomater. 2014 (2014) 1–6.
[11] M. Shahrousvand, G. Mir Mohamad Sadeghi, A. Salimi, M. Nourany, Bulk synthesis of monodisperse and highly biocompatible poly (ε-caprolactone)-diol by transesterification side-reactions, Polym.-Plast. Technol. Eng. 57 (6) (2018) 492–499.
[12] M.F. Abazari, S. Torabinejad, S. Zare Karizi, S.E. Enderami, H. Samadian, N. Hajati-Birgani, S. Norouzi, F. Nejati, A. Al bahash, V. Mansouri, Promoted osteogenic differentiation of human induced pluripotent stem cells using composited polycaprolactone/polyvinyl alcohol/carbopol nanofibrous scaffold, J. Drug Deliv. Sci. Technol. 71 (2022) 103318.
[13] V.A. Reyna-Urrutia, M. Estevez, A.M. Gonzalez-Gonzalez, R. Rosales-Ibanez, 3D scaffolds of caprolactone/chitosan/polyvinyl alcohol/hydroxyapatite stabilized by physical bonds seeded with swine dental pulp stem cell for bone tissue engineering, J. Mater. Sci. Mater. Med. 33 (12) (2022) 81.
[14] S. Uma Maheshwari, V.K. Samuel, N. Nagiah, Fabrication and evaluation of (PVA/HAp/PCL) bilayer composites as potential scaffolds for bone tissue regeneration application, Ceram. Int. 40 (6) (2014) 8469–8477.
[15] N. Baheiraei, M. Azami, H. Hosseinkhani, Investigation of magnesium incorporation within gelatin/calcium phosphate nanocomposite scaffold for bone tissue engineering, Intel J Appl CeramTechnol 12 (2) (2015) 245–253.
[16] D.E. Radulescu, O.R. Vasile, E. Andronescu, A. Ficai, Latest research of doped hydroxyapatite for bone tissue engineering, Int. J. Mol. Sci. 24 (17) (2023) 13157.
[17] S. Shahi, F. Dehghani, E.D. Abdolahinia, S. Sharifi, E. Ahmadian, M. Gajdács, K. Kárpáti, S.M. Dizaj, A. Eftekhari, T. Kavetskyy, Effect of gelatinous spongy scaffold containing nano-hydroxyapatite on the induction of odontogenic activity of dental pulp stem cells, J. King Saud Univ. Sci. 34 (8) (2022) 102340.
[18] L. Guo, X. Guo, Y. Leng, J.C. Cheng, X. Zhang, Nanoindentation study of interfaces between calcium phosphate and bone in an animal spinal fusion model, J. Biomed. Mater. Res. 54 (4) (2001) 554–559.
[19] G. Perumal, P.M. Sivakumar, A.M. Nandkumar, M. Doble, Synthesis of magnesium phosphate nanoflakes and its PCL composite electrospun nanofiber scaffolds for bone tissue regeneration, Mater. Sci. Eng., C 109 (2020) 110527.
[20] C. Mardziah, S. Ramesh, H. Chandran, A. Sidhu, S. Krishnasamy, Properties of sintered zinc hydroxyapatite bioceramic prepared using waste chicken eggshells as calcium precursor, Ceram. Int. 49 (8) (2023) 12381–12389.
[21] B. Alhussary, G.A. Taqa, A. Taqa, Preparation and characterization of natural nano hydroxyapatite from eggshell and seashell and its effect on bone healing, J Appl Vet Sci 5 (2) (2020) 25–32.
[22] V. Hembrick-Holloman, T. Samuel, Z. Mohammed, S. Jeelani, V.K. Rangari, Ecofriendly production of bioactive tissue engineering scaffolds derived from egg- and sea-shells, J. Mater. Res. Technol. 9 (6) (2020) 13729–13739.
[23] M.S. Firdaus Hussin, H.Z. Abdullah, M.I. Idris, M.A. Abdul Wahap, Extraction of natural hydroxyapatite for biomedical applications-A review, Heliyon 8 (8) (2022) e10356.
[24] L. Liu, C. Li, Y. Jiao, G. Jiang, J. Mao, F. Wang, L. Wang, Homogeneous organic/inorganic hybrid scaffolds with high osteoinductive activity for bone tissue engineering, Polym. Test. 91 (2020) 106798.
[25] A. Shafiu Kamba, Z.A.B. Zakaria, Osteoblasts growth behaviour on bio-based calcium carbonate aragonite nanocrystal, BioMed Res. Int. 2014 (2014).
[26] P. Zahedi, I. Rezaeian, S.H. Jafari, Z. Karami, Preparation and release properties of electrospun poly (vinyl alcohol)/poly (ε-caprolactone) hybrid nanofibers: optimization of process parameters via D-optimal design method, Macromol. Res. 21 (2013) 649–659.
[27] P. Zahedi, I. Rezaeian, S.H. Jafari, In vitro and in vivo evaluations of phenytoin sodium-loaded electrospun PVA, PCL, and their hybrid nanofibrous mats for use as active wound dressings, J. Mater. Sci. 48 (8) (2012) 3147–3159.

[28] P. Zahedi, M. Fallah-Darrehchi, Electrospun egg albumin-PVA nanofibers containing tetracycline hydrochloride: morphological, drug release, antibacterial, thermal and mechanical properties, Fibers Polym. 16 (2015) 2184–2192.
[29] H. Jafari, M. Shahrousvand, B. Kaffashi, Preparation and characterization of reinforced poly (ε-caprolactone) nanocomposites by cellulose nanowhiskers, Polym. Compos. 41 (2) (2020) 624–632.
[30] R.A. Alabdali, T.F. Garrison, M.M. Mahmoud, D.B. Ferry, Z.C. Leseman, Micromechanical characterization of continuous fiber date palm composites, J. Nat. Fibers 20 (2) (2023) 2280050.
[31] H. Jafari, M. Shahrousvand, B. Kaffashi, Reinforced poly (ε-caprolactone) bimodal foams via phospho-calcified cellulose nanowhisker for osteogenic differentiation of human mesenchymal stem cells, ACS Biomater. Sci. Eng. 4 (7) (2018) 2484–2493.
[32] M. Shahrousvand, G.M.M. Sadeghi, E. Shahrousvand, M. Ghollasi, A. Salimi, Superficial physicochemical properties of polyurethane biomaterials as osteogenic regulators in human mesenchymal stem cells fates, Colloids Surf. B Biointerfaces 156 (2017) 292–304.
[33] P. Ghaffari-Bohlouli, H. Jafari, A. Khatibi, M. Bakhtiari, B. Tavana, P. Zahedi, A. Shavandi, Osteogenesis enhancement using poly (l-lactide-co-d, l-lactide)/poly (vinyl alcohol) nanofibrous scaffolds reinforced by phospho-calcified cellulose nanowhiskers, Int. J. Biol. Macromol. 182 (2021) 168–178.
[34] M. Shahrousvand, M. Ghollasi, A.A.K. Zarchi, A. Salimi, Osteogenic differentiation of hMSCs on semi-interpenetrating polymer networks of polyurethane/poly (2-hydroxyethyl methacrylate)/cellulose nanowhisker scaffolds, Int. J. Biol. Macromol. 138 (2019) 262–271.
[35] H.K. Kiranda, R. Mahmud, D. Abubakar, Z.A. Zakaria, Fabrication, characterization and cytotoxicity of spherical-shaped conjugated gold-cockle shell derived calcium carbonate nanoparticles for biomedical applications, Nanoscale Res. Lett. 13 (2018) 1–10.
[36] N.I. Zakaria, R. Mohammad, S.A. Hanifah, K.H. Kamarudin, A. Ahmad, Low cost and eco-friendly nanoparticles from cockle shells as a potential matrix for the immobilisation of urease enzyme, Arab. J. Chem. 14 (4) (2021) 103056.
[37] S.K. Mahmood, M.Z.A.B. Zakaria, I.S.B.A. Razak, L.M. Yusof, A.Z. Jaji, I. Tijani, N.I. Hammadi, Preparation and characterization of cockle shell aragonite nanocomposite porous 3D scaffolds for bone repair, Biochemistry and biophysics reports 10 (2017) 237–251.
[38] E. Sinurat, F. Dewi, D. Fransiska, R. Nurbayasari, Synthesis and characterization of hydroxyapatite of cockle shells (anadara granosa) originated from Indonesia through precipitation method, in: IOP Conference Series: Earth and Environmental Science, IOP Publishing, 2022 012035.
[39] S.F.S. Mohamad, S. Mohamad, Z. Jemaat, Study of calcination condition on decomposition of calcium carbonate in waste cockle shell to calcium oxide using thermal gravimetric analysis, ARPN J. Eng. Appl. Sci. 11 (16) (2016) 9917–9921.
[40] S.S. Ghazali, K.L. Kem, R. Jusoh, S. Abdullah, J.H. Shariffuddin, Evaluation of La-doped CaO derived from cockle shells for photodegradation of POME, Bull. Chem. React. Eng. Catal. 14 (1) (2019) 205–218.
[41] B. Ghanshyam, S. Sonawane Shriram, L. Wasewar Kailas, P. Rathod Ajit, R. Parate Vishal, H. Sonawane Shirish, G. Shimpi Navin, Improvement in thermal stability, thermomechanical and oxygen permeability of PA6 by ODA modified Ca3 (PO4) 2 nanofiller, Res. J. Chem. Environ. 21 (6) (2016) 38–44.
[42] S. Pourbashir, M. Shahrousvand, M. Ghaffari, Preparation and characterization of semi-IPNs of polycaprolactone/poly (acrylic acid)/cellulosic nanowhisker as artificial articular cartilage, Int. J. Biol. Macromol. 142 (2020) 298–310.
[43] F.A. Sheikh, N.A. Barakat, M.A. Kanjwal, S.J. Park, D.K. Park, H.Y. Kim, Synthesis of poly (vinyl alcohol)(PVA) nanofibers incorporating hydroxyapatite nanoparticles as future implant materials, Macromol. Res. 18 (2010) 59–66.
[44] A.S. Asran, S. Henning, G.H. Michler, Polyvinyl alcohol–collagen–hydroxyapatite biocomposite nanofibrous scaffold: mimicking the key features of natural bone at the nanoscale level, Polymer 51 (4) (2010) 868–876.
[45] P. Zahedi, Z. Karami, I. Rezaeian, S.-H. Jafari, P. Mahdaviani, A.H. Abdolghaffari, M. Abdollahi, Preparation and performance evaluation of tetracycline hydrochloride loaded wound dressing mats based on electrospun nanofibrous poly(lactic acid)/poly(ε-caprolactone) blends, J. Appl. Polym. Sci. 124 (5) (2012) 4174–4183.
[46] B. Motealleh, P. Zahedi, I. Rezaeian, M. Moghimi, A.H. Abdolghaffari, M.A. Zarandi, Morphology, drug release, antibacterial, cell proliferation, and histology studies of chamomile-loaded wound dressing mats based on electrospun nanofibrous poly(varepsilon-caprolactone)/polystyrene blends, J. Biomed. Mater. Res. B Appl. Biomater. 102 (5) (2014) 977–987.
[47] L.F. Bonewald, Osteocytes, Marcus and Feldman's Osteoporosis (2021) 135–163. Elsevier.
[48] X. Luo, Z. Guo, P. He, T. Chen, L. Li, S. Ding, H. Li, Study on structure, mechanical property and cell cytocompatibility of electrospun collagen nanofibers crosslinked by common agents, Int. J. Biol. Macromol. 113 (2018) 476–486.
[49] S. Mahalingam, C. Bayram, M. Gultekinoglu, K. Ulubayram, S. Homer-Vanniasinkam, M. Edirisinghe, Co-axial gyro-spinning of PCL/PVA/HA core-sheath fibrous scaffolds for bone tissue engineering, Macromol. Biosci. 21 (10) (2021) e2100177.
[50] M. Shahrousvand, M.S. Hoseinian, M. Ghollasi, A. Karbalaeimahdi, A. Salimi, F.A. Tabar, Flexible magnetic polyurethane/Fe2O3 nanoparticles as organic-inorganic nanocomposites for biomedical applications: properties and cell behavior, Mater. Sci. Eng. C 74 (2017) 556–567.
[51] M. Shahrousvand, N.G. Ebrahimi, Designing nanofibrous poly (ε-caprolactone)/hydroxypropyl cellulose/zinc oxide/Melilotus Officinalis wound dressings using response surface methodology, Int. J. Pharm. 629 (2022) 122338.
[52] P. Askari, P. Zahedi, I. Rezaeian, Three-layered electrospun PVA/PCL/PVA nanofibrous mats containing tetracycline hydrochloride and phenytoin sodium: a case study on sustained control release, antibacterial, and cell culture properties, J. Appl. Polym. Sci. 133 (16) (2016).
[53] J. Chen, Z.-D. Shi, X. Ji, J. Morales, J. Zhang, N. Kaur, S. Wang, Enhanced osteogenesis of human mesenchymal stem cells by periodic heat shock in self-assembling peptide hydrogel, Tissue Eng. 19 (5–6) (2013) 716–728.
[54] J. López-García, M. Lehocký, P. Humpolíček, P. Sáha, HaCaT keratinocytes response on antimicrobial atelocollagen substrates: extent of cytotoxicity, cell viability and proliferation, J. Funct. Biomater. 5 (2) (2014) 43–57.
[55] S. Gautam, C. Sharma, S.D. Purohit, H. Singh, A.K. Dinda, P.D. Potdar, C.F. Chou, N.C. Mishra, Gelatin-polycaprolactone-nanohydroxyapatite electrospun nanocomposite scaffold for bone tissue engineering, Mater. Sci. Eng., C 119 (2021) 111588.
[56] L.F. Mellor, R.C. Nordberg, P. Huebner, M. Mohiti-Asli, M.A. Taylor, W. Efird, J.T. Oxford, J.T. Spang, R.A. Shirwaiker, E.G. Loboa, Investigation of multiphasic 3D-bioplotted scaffolds for site-specific chondrogenic and osteogenic differentiation of human adipose-derived stem cells for osteochondral tissue engineering applications, J. Biomed. Mater. Res. B Appl. Biomater. 108 (5) (2020) 2017–2030.
[57] R. Didekhani, M.R. Sohrabi, M. Soleimani, E. Seyedjafari, H. Hanaee-Ahvaz, Incorporating PCL nanofibers with oyster shell to improve osteogenic differentiation of mesenchymal stem cells, Polym. Bull. 77 (2) (2019) 701–715.
[58] Yudyanto Hartatiek, M.I. Wuriantika, J. Utomo, M. NurhudaMasruroh, D.J.D.H. Santjojo, Nanostructure, porosity and tensile strength of PVA/Hydroxyapatite composite nanofiber for bone tissue engineering, Mater. Today: Proc. 44 (2021) 3203–3206.